

TARGET IONIZATION DYNAMICS BY IRRADIATION OF X-RAY FREE-ELECTRON LASER LIGHT

Tatsufumi Nakamura*, Yuji Fukuda

Kansai Photon Science Institute, JAEA, Kyoto, Japan

Yasuaki Kishimoto, Graduate school of Energy Science, Kyoto University, Kyoto, Japan

Abstract

Interactions of x-ray free electron laser (XFEL) light with a single cluster target are numerically investigated by using a three-dimensional Particle-in-Cell code. The plasma dynamics as well as relevant atomic processes are taken into account, such as photo-ionization, the Auger effect, collisional ionization/relaxation, and field ionization. It is found that as the XFEL intensity increases to as high as $\sim 10^{21}$ photons/pulse/mm², the field ionization becomes the dominant ionization process over the other atomic processes. The target damage due to the irradiation by XFEL light is numerically evaluated, which gives an estimation of the XFEL intensity so as to suppress the target damage within a tolerable range for imaging.

INTRODUCTION

X-ray free electron lasers (XFEL), which are emerging in a couple of years in Europe, the US and Japan [1, 2, 3], provide extremely high flux of coherent x-rays such as $10^{20} \sim 10^{22}$ photons/pulse/mm², with a photon energy of ~ 12 keV and pulse length of ~ 10 fs. The XFEL light is expected to realize diffractive imaging with high resolution, of material and especially biological samples such as living cells. The high flux of x-rays enables single shot imaging of a target without crystallization, but at the same time leads to target damage due to the rapid ionization and resultant ion movement by plasma expansion. Therefore, it is an important issue to explore the ionization dynamics of the target by the irradiation of intense XFEL light. The interactions of intense x-rays with matter have been intensively studied experimentally [4] and theoretically. Theoretical approaches are carried out by using various methods such as quantum-classical simulations [5], hydrodynamics simulations [6], and molecular dynamics simulations [7]. In the above analyses, the dynamics of target ions and molecules are analyzed by taking into account atomic processes, such as photo-ionization, the Auger effect, and collisional ionization. However, the ionization by an electric field and its enhancement due to the dynamics of the high energy electrons, generated by the photo-ionization process and having roughly the same energy as the incident photon, are neglected or partially treated. More precisely, collisional ionization by high energy electrons are treated, but less attention has been paid on the plasma dynamics. The formation of strong electric field leads to the rapid ionization of the target, which is induced by electrons escaped from the cluster potential and enhanced by the sheath field.

In this paper, we analyze the ionization dynamics of cluster targets irradiated by intense XFEL light by using a three-dimensional particle-in-cell (PIC) code in order to take into account the plasma dynamics as well as atomic processes such as photo-ionization, the Auger effect, and collisional ionization/relaxation [8]. It is shown that as the incident XFEL intensity increases to $\sim 10^{21}$ photons/pulse/mm² field ionization plays a dominant role in ionization processes and leads to the rapid ionization of the target. The average number of bound electrons per atom during XFEL irradiation is evaluated, which gives us the estimation of the upper limit of XFEL intensity for suppressing the target damage within a tolerable range.

NUMERICAL MODELING

The relevant ionization processes of a target irradiated by XFEL light are modeled as follows. At first, incident x-ray photons ionize the target via inner-shell ionization. This is due to the fact that the cross section of photo-ionization is dominated by that of inner-shell ionization for the wavelength of 0.1 nm [9]. The photo-ionization process results in the generation of a high energy electron (~ 12 keV) and an unstable hollow atom where a K-shell electron is removed. The relaxation of the unstable atom is achieved by a L-shell electron falling into the vacant orbital, and its energy is given to another electron, *i.e.*, the target is further ionized, which is known as the Auger process. The target ionization also proceeds by the Coulomb collisions and the electric field induced by high energy electrons. The whole ionization dynamics of the target is determined by the competition of the above ionization processes depending on the laser and target parameters, which is explored in the next section for the parameter regime being relevant to XFEL light interacting with bio-molecules.

In our PIC code, EPIC3D [10], the above processes are treated in the following way. The wave propagation of x-ray is not solved in the simulations. The interaction between the x-rays and the target is treated through photo-ionization events. The atoms in the target are set to be ionized at the ionization rate which is calculated from the cross section of inner-shell ionization, *e.g.*, $\sigma_{222-122} = 2.1147 \times 10^{-23}$ cm² for an incident photon of 0.1 nm wavelength [9], where 222-122 means that the electronic state of the initial and final state are $1s^2 2s^2 2p^2$ and $1s^1 2s^2 2p^2$. The information of the electronic state is assigned to each atom, which makes it possible to treat the generation of hollow atoms and the Auger effect. The Auger effect is treated as an ionization event of the atoms with a certain time interval after the excitation, which is determined by

* nakamura.tatsufumi@jaea.go.jp

the life time of the unstable excited state, *e.g.*, $\tau = 28.57$ fs for the transition from $1s2s^22p$ to $1s^22p$, $\tau = 14.14$ fs for $1s2s^2-1s^2$, and so on [11]. Ionizations by electric field is modeled by Monte Carlo method, where an atom is ionized when $1 - \exp(-\nu\Delta t) \geq \alpha$. Here, Δt , α and ν are time step in the simulation, uniform random number in $[0,1]$ and the ionization rate, respectively. The ionization rate is calculated by using the ADK formula [12], which depends on the local electric field, binding energy of the electron, and a set of quantum numbers, *i.e.*, the effective principal n , orbital quantum number ℓ , and its projection m . Relaxation processes by electron-electron, electron-ion, and ion-ion collisions are also taken into account, where binary collisions are calculated by making particle pairs following the method of Takizuka and Abe [13]. The ionization by electron collision is also calculated in the same manner as field ionization with ionization rate calculated by using the BEB formula [14]. The radiative and three-body recombination processes are not taken into account, which are less effective in time scale of XFEL irradiation which is tens of femto-second.

TARGET IONIZATION BY XFEL IRRADIATION

We consider the ionization dynamics of a carbon cluster target to model a protein molecule which is irradiated by intense XFEL light. The simulation condition is as follows. The target is a spherical carbon cluster with atomic density of $n_0 = 3.0 \times 10^{22}/\text{cm}^3$ and a diameter of 20 nm, which are comparable to a standard bio-molecule sample. The simulation box size is $128\text{nm} \times 128\text{nm} \times 128\text{nm}$ with mesh size of 1 nm. 3.7×10^5 particles are used for carbon atom, which is half of the real number of atoms. Absorbing boundary conditions are adopted for both the particles and fields. The XFEL intensity is 10^{22} photons/pulse/ mm^2 with a wavelength of 0.1 nm. The pulse length is 10 fs with a Gaussian distribution. A simulation with larger system size with $192\text{nm} \times 192\text{nm} \times 192\text{nm}$, and a simulation with twice the finer mesh size are performed and we confirmed that the system size and mesh size do not affect the results.

The two-dimensional distribution of the electrostatic field and electron density at $t = 6$ fs are shown in Fig. 1(a) and 1(b), respectively, and their radial distribution is plotted in Fig. 1(c). The electric field intensity is highest at the surface which is of the order of TV/m, and one order smaller ~ 0.1 TV/m on the inner side of the target. The electric field is not stationary but evolves in time as a result of electrons and ions motion. At first, the electric field is induced by electrons which escaped from the cluster until the potential reaches to 12 keV of photo-electron energy. This electric field is estimated by equating photo-electron energy with electro-static potential,

$$e\phi = \frac{eN^s}{4\pi\epsilon_0 R} \sim 12\text{keV} \quad (1)$$

, where e, ϵ_0, R, N^s are electron charge, dielectric con-

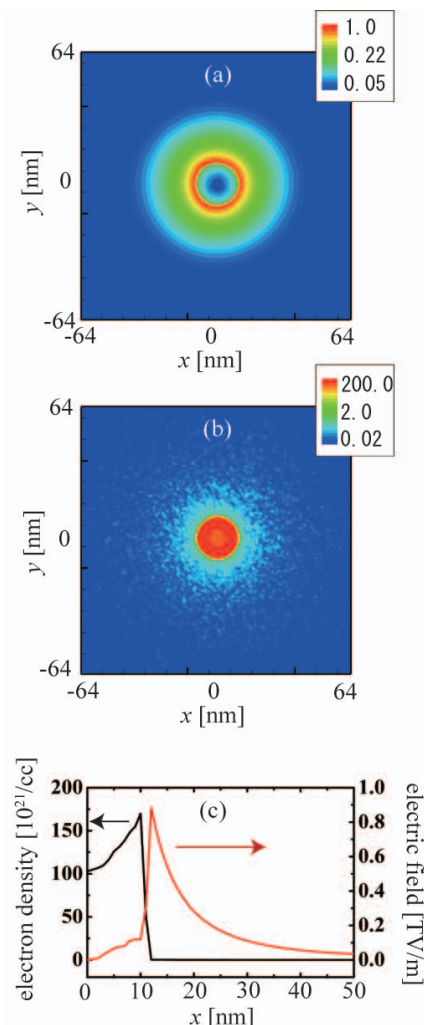


Figure 1: Two-dimensional distribution of the electron density in units of $10^{22}/\text{cm}^3$. The plane is chosen at $z=0$, *i.e.* the cluster center corresponds to the origin of the $x-y$ plane. (b) Two-dimensional distribution of the electric field in units of TV/m. (c) Line distribution along x -coordinate $x \geq 0$. (d) Temporal evolution of maximum intensity of electric field.

stant, cluster radius and number of electrons escaped from the cluster, respectively. For the cluster with radius of 10nm, eq. (1) leads to $N^s \sim 8 \times 10^4$. By solving the rate equation, it is calculated that the number of photo-ionized electrons becomes N^s at $t = 6.1$ fs. When N^s electrons have escaped, the electro-static potential begins to trap the electrons around the cluster and the electro-static field of $E = eN^s/4\pi\epsilon_0 R^2 \sim 1.2\text{TV/m}$ is induced, which is achieved at $t \sim 7$ fs. After the cluster is charged-up, roughly 1.7×10^5 K-shell electrons are not yet ionized. When these K-shell electrons are photo-ionized, they are confined around the cluster with slight expansion and resultant charge separation induces the electric field at the cluster surface, which is known as a sheath field, which further ionizes the target.

From the perspective of bio-molecule imaging using XFEL light, target ionization is desired to be suppressed

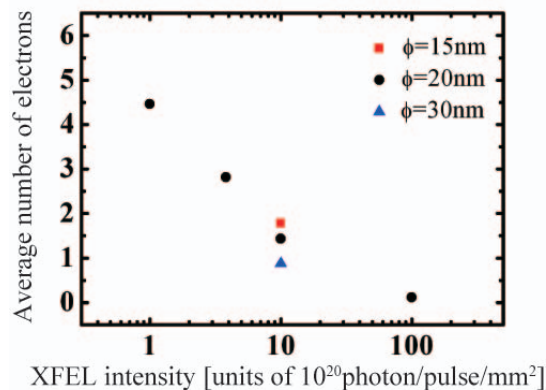


Figure 2: The time history of the ion energy spectra accelerated by the x-ray interaction with a carbon cluster.

as much as possible since it is the bound electrons that generate diffraction patterns of the target structure. Considering that the sheath field intensity is proportional to $\sqrt{n_h}$, the crucial ionization process is suppressed by lowering the XFEL intensity. In order to derive a criteria of tolerable target damage, we performed simulations for different XFEL intensities. The target damage was numerically evaluated by introducing the average number of bound electrons per atom defined by

$$\overline{N_e} = \frac{\int \langle N_e(t) \rangle I(t) dt}{\int I(t) dt}, \quad (2)$$

where $\langle \rangle$ denotes an ensemble average over the atoms. The time-average is calculated by the time-integration with a weighting of $I(t)$ which denotes the temporal dependence of the incident XFEL light, since the diffraction signal is proportional to the incident XFEL light intensity. The results are summarized in Fig. 2. The bound electron number sharply decreases with increasing XFEL intensity. As the XFEL intensity becomes higher than 10^{21} photon/pulse/mm 2 , the average number of bound electrons becomes less than one, which means that atoms are completely ionized or barely hold one electron. As the intensity decreases down to 10^{20} photon/pulse/mm 2 , there exists 4 ~ 5 electrons in each atom which seems favorable for imaging. In the above simulations, the pulse length is set to be 10 fs which is the current design parameter of the XFEL in Japan, because this time scale is shorter than the life time of the Auger ionization of inner-shell ionized carbon atoms. Since the hot electron number density is determined by the total number of incident photons, the laser pulse length does not change the total numbers of ionization events as far as the total photon number is kept constant. If the pulse length is longer, *e.g.*, twice, the temporal evolution of the field ionization is stretched, *e.g.*, a factor of two. But the field intensity and resulting ionization by the field do not change a lot, and the Auger effect and collisional ionization becomes to work more effectively. To summarize, when irradiating XFEL light onto a solid density target for single shot imaging, the XFEL light source is made to be shorter than 10 fs in order to prevent target ionization by the Auger effect. In addition to this condi-

tion, it is found that it is desirable for the XFEL intensity to be lower than 10^{20} photon/pulse/mm 2 to prevent rapid ionization via field ionization. Alternatively, the XFEL light source should be further shortened such as towards the attosecond regime in order to finish the interaction before the field ionization takes place.

CONCLUSION

In conclusion, we have performed numerical analyses on the interaction of XFEL light with a cluster target by the developed PIC code. It is shown that field ionization plays a dominant role in the ionization dynamics as the XFEL intensity increases up to 10^{21} photons/pulse/mm 2 . The field ionization leads to the rapid and spatially non-uniform ionization of the target, which leads to the fact that highly charged ions are generated in the cluster from the outer shell. To prevent the serious target damage, the XFEL light source should be made to suppress the field ionization as well as the Auger ionization. From the numerical evaluation, it is indicated that it is desirable for the XFEL laser pulse with intensity less than 10^{20} photons/pulse/mm 2 or much shorter pulse duration of attosecond regime.

REFERENCES

- [1] The European X-ray Laser Project XFEL; <http://xfel.desy.de>
- [2] XFEL project in US; <http://www-ssrl.slac.stanford.edu/1c1s>
- [3] XFEL project in Japan; <http://www.riken/jp/XFEL/eng/index.html>
- [4] T. Laarmann, M. Rusek, H. Wabnitz *et al.*, Phys. Rev. Lett. **95**, 0634021 (2005); H. Wabnitz, A.R.B. de Castro, P. Gürtler *et al.*, Phys. Rev. Lett. **94**, 133401 (2005).
- [5] S.P. Hau-Riege, R.A. London, A. Szoke, Phys. Rev. E **69**, 051906 (2004); I. Georgescu, U. Saalman, J. Rost, Phys. Rev. A **76**, 043203 (2007).
- [6] M. Rusek, A. Orłowski, Phys. Rev. A **71**, 043202 (2005).
- [7] R. Neutze, R. Wouts, D. van der Spoel *et al.*, Nature **406**, 752 (2000); Z. Jurek, M. Tange, Eur. Phys. J. D **29**, 217 (2004); C. Jungreuthmayer, L. Ramunno, J. Zanghellini *et al.*, J. Phys. B: At. Mol. Opt. Phys. **38**, 3029 (2005).
- [8] T. Nakamura, Y. Fukuda, Y. Kishimoto, Phys. Rev. A **80**, 053202 (2009).
- [9] B.L. Henke, E.M. Gullikson, J.C. Davis, Atomic Data Nucl. Data Tables **54**, 181 (1993).
- [10] Y. Kishimoto, Annual Report of the Earth Simulator Center, Apr. 2003-March 2005, pp.199 (2004).
- [11] K. Moribayashi, J. Phys. B: At. Mol. Opt. Phys. **41**, 085602 (2008).
- [12] M.V. Ammosov, N.B. Delone, V.P. Krainov, Sov. Phys. JETP, **64**, 1191, (1986).
- [13] T. Takizuka, H. Abe, J. Comp. Phys. **25**, 205 (1977); Y. Sentoku, K. Mima, Y. Kishimoto *et al.*, J. Phys. Soc. Jpn. **67**, 4084 (1998).
- [14] Y.K. Kim, M.E. Rudd, Phys. Rev. A **50**, 3954 (1994).